Cell and Tissue Research (2019) 375:397–408
https://doi.org/10.1007/s00441-018-2920-0

REGULAR ARTICLE

Enrichment of cancer stem cells by agarose multi-well dishes and 3D spheroid culture

Xiaoling Guo[1] · Yong Chen[1] · Weiping Ji[2] · Xianwu Chen[1] · Chao Li[1] · Renshan Ge[1,3]

Received: 22 November 2017 / Accepted: 5 September 2018 / Published online: 22 September 2018

Abstract

As the theory of cancer stem cells (CSCs) is maturing, CSC-targeted therapy is emerging as an important therapeutic strategy and seeking the ideal method for rapid enrichment and purification of CSCs has become crucial. So far, based on the known CSC phenotypes and biological characteristics, the methods for enrichment CSCs mainly include low adhesion culture, low oxygen culture, chemotherapy drug stimulation and side population (SP) sorting but these methods cannot realize quick enrichment of the desired CSCs. Herein, we adopt a novel method that efficiently enriches a certain amount of CSCs through agarose multi-well dishes using rubber micro-molds to make cancer cells into cell spheroids (3D). These 3D cancer cell spheroids in the proportions of expression of CSC biomarkers (single stain of CD44, CD44v6 and CD133 or double stain of both CD44 and CD133) were significantly higher than those of the conventional adherent culture (2D) using flow cytometry analysis. In addition, the expression levels of stemness transcription factors such as OCT4, NANOG and SOX2 in 3D were also significantly higher than that in 2D through Western blot (WB) and quantitative polymerase chain reaction (qPCR) assays. In addition, the CSCs in 3D could form colonies with different sizes in soft agar. In conclusion, we developed a new method to enrich some kinds of CSCs, which might be a benefit for future CSC-targeted therapy studies and anti-CSC drug screening applications.

Keywords Cancer stem cell · 2D · 3D · Spheroid · Enrichment

Introduction

Cancer is the leading cause of death in economically developed countries and the second leading cause of death in developing countries, which is an increasing medical burden worldwide, due to population growth (Jemal et al. 2011). Recently, cancer stem cell (CSC) theory has attracted much attention. The CSC hypothesis originated in the late nineteenth century and the existence of CSCs was demonstrated a century later (Sell 2004). Studies have revealed that CSCs are a rare cell population in blood cancers and solid tumors. CSCs in blood cancer were first identified in acute myeloid leukemia in 1997 (Bonnet and Dick 1997) and the first CSCs in solid tumors were identified in breast cancer in 2003 (Al-Hajj et al. 2003). So far, CSCs have been isolated from most solid tumors, including breast cancer (Velasco-Velazquez et al. 2012), ovarian cancer (Meirelles et al. 2012), prostate cancer (Salmanzadeh et al. 2012), colon cancer (O'Brien et al. 2007), brain cancer (Singh et al. 2003), pancreatic cancer (Li et al. 2009) and melanoma (Schatton et al. 2008).

CSCs have similar properties to adult stem cells with the ability of unlimited self-renewal and differentiation (Clarke et al. 2006). The tumorigenic ability of CSCs is strong and just as few as 500 CSCs from the PLC/PRF/5 spheres were able to form a tumor when subcutaneously injected into NOD/SCID mice (Cao et al. 2011). CSCs appear to be highly resistant to various chemotherapies such as doxorubicin, fluorouracil, cyclophosphamide, etoposide and cisplatin (Zhang et al. 2012) as well as radiation (Lopez et al. 2012). CSCs can be successfully isolated and enriched mainly based on

Xiaoling Guo and Yong Chen contributed equally to this work.

✉ Renshan Ge
r_ge@yahoo.com

[1] Center of Scientific Research, The Second Affiliated Hospital and Yuying Children's Hospital of Wenzhou Medical University, Wenzhou, China

[2] Department of Gastroenetrology, The Second Affiliated Hospital and Yuying Children's Hospital of Wenzhou Medical University, Wenzhou, China

[3] Department of Anesthesiology, The Second Affiliated Hospital and Yuying Children's Hospital of Wenzhou Medical University, 109 Xueyuan West Road, Wenzhou 325027, Zhejiang, China

their specific cell surface phenotypes, specifically CD44, CD133, CD44v6, CD34, epithelial cell adhesion molecule (EpCAM) and CD13, which are involved in embryonic and somatic stem cell function and embryonic development (Ricci-Vitiani et al. 2007; Takaishi et al. 2009).

Cancer is traditionally treated using surgical resection, chemotherapy and fractionated radiotherapy. However, off-target effects, treatment-related side effects and drug resistance limit the efficacy of many therapeutic options (Zhang et al. 2017). CSCs are a major source of cancer initiation, progression and drug resistance for tumor recurrence (Lee et al. 2017b; Peitzsch et al. 2017; Wang et al. 2017). Therefore, exploration of novel methods to rapidly enrich CSCs for CSC-targeted therapy studies and anti-CSC drug screening applications to eliminate cancer become extremely important. So far, according to the characteristics of CSCs, there are several methods for enrichment of CSCs such as low adhesion culture (Wang et al. 2012), low oxygen culture (Bhaskara et al. 2012), chemotherapy drug stimulation (Hu et al. 2012) and side population (SP) sorting (Chien et al. 2012). However, these methods cannot achieve the rapid enrichment of a certain amount of CSCs. The present study systematically elaborates a new simple and rapid method for the enrichment of some kinds of CSCs, which might be used as a potential supplement for cancer stem cell enrichment.

Materials and methods

Culture of cancer cells

Cancer cells such as human ovarian mucosal cells (OVCAR-3), human colon cancer cells (SW620), human pancreatic cancer cells (PANC-1), and human prostate cancer cells (PC3) were separately seeded into 6-well culture plates with a density of 2×10^4 cells/well and incubated in a 37 °C, 5% CO_2 incubator. The culture medium contained 5% fatal bovine serum (FBS), 1% penicillin and streptomycin (P/S) and DMEM/F12 (Gibco, NY, USA). The medium was changed every 2 days. When cancer cells reached 100% confluence, they were passaged by 0.25% EDTA-trypsin (Gibco) for the conventional adherent culture (2D) and cell spheroid culture (3D). For the following experiments, the mediums of cancer cells in 2D or 3D were changed into DMEM/F12 with 10 μM Y-27632 (Sigma, MO, USA), 5% FBS, 2% HS (Gibco), 1% P/S.

Preparation of agarose micro multi-well dishes and 3D cancer cell spheroids

Eighty-one-well rubber micro-molds (Fig. 1a) with a diameter of 400 μm were purchased from Micro Tissues Inc. (Providence, RI, USA). Molds were sterilized with anhydrous ethanol and allowed to dry in an ultraviolet irradiation environment for 1 h. Two percent (g/ml) agarose powder (Sigma) was mixed with DMEM/F12 and then the solution was autoclaved sterilization. When the solution was still liquid, 500 μL of solution was pipetted into each mold (Fig. 1a′). After solidification, the micro-well plates were removed with a sterilized shovel (Fig. 1a″). The agarose dishes were equilibrated in 6-well culture Petri dishes (Corning, NY, USA) with 2 mL DMEM/F12 containing 1% P/S in a 37 °C incubator of 5% CO_2, for 24 h (Fig. 1b). Before seeding cancer cells into the micro-well plates, the medium was removed from both the culture dishes and the micro-well plates. Then, 200 μL cell suspension containing 5×10^5 cells/mL was carefully seeded into each well of the micro-well plates and 2 mL DMEM/F12 with 10 μM Y-27632, 5% FBS, 2% HS and 1% P/S was pipetted into 6-well culture Petri dishes. The culture dishes were incubated in a 37 °C incubator of 5% CO_2 and the medium was changed every 2 days. After 4 days, almost all cancer cells were generated into spheroids (Fig. 1b′), which were then harvested for the following experiments or carefully transferred to new non-adhesive plastic Petri dishes (Corning) for obtaining cancer cell spheroid images (Fig. 1b″).

Soft agar colony formation assay

For the soft agar assay, the above collected cancer cell spheroids (about 80 μm diameter) were pretreated for 20 min using 0.25% EDTA trypsin in a 37 °C, 5% CO_2 incubator for the preparation of cell suspension and then the dissociated cells, a total of 1×10^4 cells, were seeded into the medium with 0.6% agarose (Sigma). The culture dishes were placed in a 37 °C incubator of 5% CO_2. The culture medium contains DMEM/F12, 10 μM Y-27632, 5% FBS, 2% HS and 1% P/S and was changed every 2 days. Colonies were formed and recorded after 14 days of growth.

Flow cytometry

The 2D and 3D cancer cells were harvested at 1500 rmp for 5 min, while cancer cell spheroids were pretreated for 20 min using 0.25% EDTA trypsin at 37 °C, 5% CO_2 incubator for the preparation of cell suspension. Then, harvested cancer cells were washed once with phosphate buffered saline (PBS, Gibco) and fixed with 4% paraformaldehyde (Sigma) at 4 °C overnight. The fixed cells were washed again with PBS and blocked with 2 mL PBS containing 5% FBS (5% FBS-PBS) at room temperature for 10 min. For single labeling, the cells were then labeled with primary or isotype control antibodies FITC-CD44, FITC-CD44v6 and APC-CD133 (BD, NJ, USA) separately in a dark place at room temperature for 20 min. For double labeling, the cells were then labeled with primary or isotype control antibodies both FITC-CD44 and APC-CD133 in a dark place at room temperature for 20 min. The labeled cells were rinsed with PBS three times

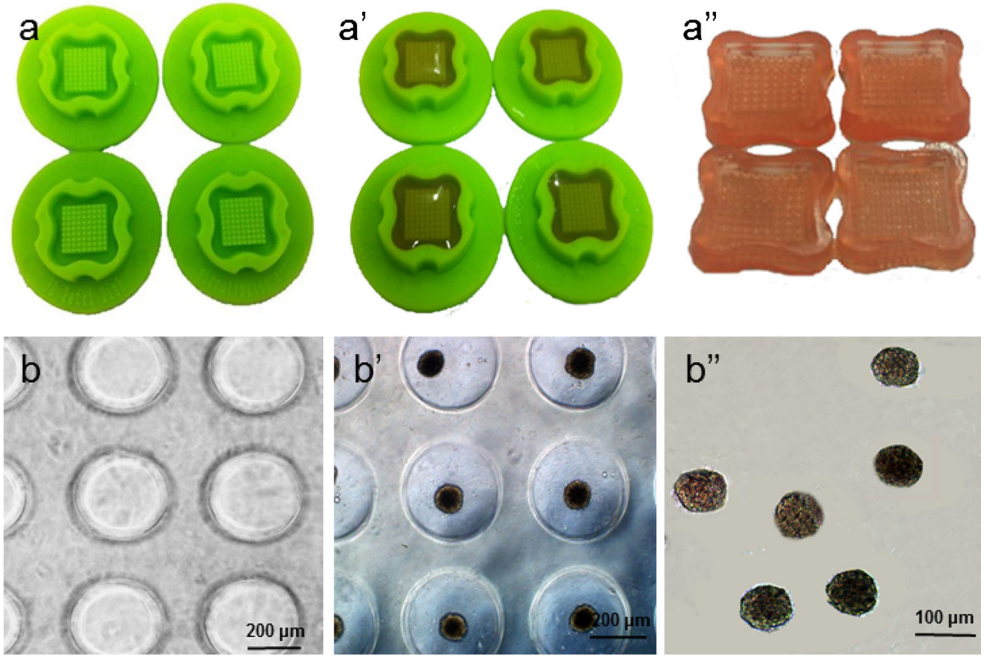

Fig. 1 Schematic of methods used in generation of cancer cell spheroids. Production of agarose 3D Petri dishes for generating cancer cell aggregates. The flexible and reusable rubber micromolds with multiple projections (a) were filled with liquid agarose (pink) (a′). After cooling, multiwell agarose culture dishes were generated (a″). The protocol used for the generation of cancer cell spheroids. (b) Observation of the agarose micromold groove type under an inverted microscope. (b′) The suspensions of cancer cells were pipetted into an agarose multiwell dish containing medium. (b″) After 4 days, aggregates were removed and transferred to a non-adhesive plastic Petri dish

for 5 min each and suspended in 500 μL PBS for detection by flow cytometry analyzer (BD). Data analysis was performed by FCS Express 4 Flow Research Edition software.

Western blot

Cells were harvested and washed once with PBS and then lysed in a radio immunoprecipitation assay buffer (RIPA) (Beyotime, Shanghai, China) supplemented with a protease inhibitor. Lysate was centrifuged at 12,000×*g* at 4 °C for 15 min. The protein concentrations in the supernatants were measured using the BCA Assay Kit (Beyotime) as per the manufacturer's instructions. Sample proteins (50 μg) were subjected to 10% polyacrylamide gel containing sodium dodecyl and then transferred into a the polyvinylidene fluoride membrane. After being blocked with 5% free-fat milk in tween 20-containing tris-buffered saline at 4 °C for 2 h, the membranes were incubated at 4 °C overnight with primary antibodies against rabbit anti-OCT4 (1:3000, Abcam, MA, USA), rabbit anti-NANOG (1:2000, Abcam) mouse anti-SOX2 (1:3000, Abcam), and rabbit anti-GADPH (1:3000, Bioworld, MN, USA). The membranes were washed with tween 20-containing tris-buffered saline for five times and incubated with horseradish peroxidase-conjugated secondary antibody (1:5000, Bioword) for 1 h at room temperature and washed with the buffer for three times. The protein bands were visualized with enhanced chemiluminescence (Pierce Chemical Co, IL, USA). The intensity of proteins was quantified using Image J software.

Quantitative polymerase chain reaction (qPCR) assays

Total RNAs from 2D and 3D cancer cells were extracted using Trizol (Invitrogen, CA, USA) and the concentration of RNA was quantified by measuring OD at 260 nm. Total RNA was incubated at 65 °C for 5 min and then on ice for 5 min. Total RNA (1 mg) was reverse transcribed in a 10 μL reaction mixture containing 0.5 μL RT Enzyme Mix, 0.5 μL Primer Mix, 2 μL 5 × RT Buffer, 6 μL nuclease-free water at 37 °C for 15 min and at 98 °C for 5 min. The cDNA was synthesized, diluted and used to perform qPCR to analyze *Oct4* gene expression level using CFX96 Real-Time PCR Detection System (Bio-Rad, CA, USA). The primers of *Oct4*, *Nanog*, *Sox2* and *Gadph* were as follows: F/*Oct4*: GAAGGATGTGGTCCGAGTGT, R/*Oct4*: AAATAATCGGGGCTG CCAGG; F/*Nanog*: CAAGAACTCTCCAACATCCTGAA, R/*Nanog*: CCTGCGTCACACCATTGCTATTC; F/*Sox2*: CAGGAGTTGTCAAGGCAGAGA, R/*Sox2*: CCGCCGCCGATGATTGTTA; F/*Gadph*: ACAACTTT GGTATCGTGGAAGG, R/*Gadph*: GCCATCA CGCCACAGTTTC. The reaction mixture consisted of 10 μL SYBR Green Mix (Biomiga, SD, USA), 0.8 μL forward, 0.8 μL reverse primers, 1 μL diluted cDNA and 7.4 μL ddH_2O. The reaction process was 95 °C for 3 min, followed by 35 cycles of 95 °C for 10 s and 59 °C for 30 s. The relative expression of the genes was normalized against GAPDH. Melting curves were examined for the quality of the PCR amplification of each sample and quantification was performed using the comparative Ct ($2^{-\Delta\Delta Ct}$) method.

Statistical analysis

All data are presented as the mean ± standard errors (SE). Statistical significance was analyzed using one-way ANOVA followed by ad hoc Tukey multiple comparisons between two groups. Statistical analyses were performed using GraphPad Prism (version 6, GraphPad Software Inc., San Diego, CA, USA). $^{*}P < 0.05$, $^{**}P < 0.01$, or $^{***}P < 0.001$ were considered statistically significant.

Results

Flow cytometry comparative analysis of cancer stem cell biomarker expressions in 2D and 3D cancer cells

Flow cytometry was used to assess the CSC biomarker expressions in cancer cells cultured in different states. The biomarkers of solid cancer stem cells mainly focused on CD series molecules, including CD133, CD44, CD34 and CD117. The expression of typical cell surface phenotypes of CD44, CD133 and CD44v6 were selected to detect the CSC proportions in 2D and 3D human ovarian mucosal cells (OVCAR-3), human colon cancer cells (SW620), human pancreatic cancer cells (PANC-1) and human prostate cancer cells (PC3) in this study.

As shown in Fig. 2 after flow cytometry, in OVCAR-3, the percentages of CD44 positive cells in 3D (15.69 ± 1.67)% and in 2D (4.91 ± 0.65)% were both higher than those of isotype control (0.05 ± 0.01)% (Fig. 2a–a″) and in 3D they were significantly higher than in 2D ($^{**}P < 0.01$) (Fig. 2b). Those of CD44v6 positive cells in 3D (10.68 ± 1.23)% and in 2D (3.24 ± 0.52)% were higher than those of the isotype control (0.58 ± 0.07)% (Fig. 2c–c″) and in 3D they were significantly higher than in 2D ($^{*}P < 0.05$) (Fig. 2d). The percentages of CD133 positive cells in 3D (10.42 ± 1.17)% and in 2D (4.10 ± 0.62)% were both higher than those of the isotype control (0.33 ± 0.04)% (Fig. 2e–e″) and in 3D they were significantly higher than in 2D ($^{*}P < 0.05$) (Fig. 2f).

As shown in Fig. 3 after flow cytometry, in SW620, the percentages of CD44 positive cells in 3D (14.07 ± 1.32)% and in 2D (7.81 ± 0.82)% were both higher than those of the isotype control (0.37 ± 0.05)% (Fig. 3a–a″) and in 3D they were significantly higher than in 2D ($^{**}P < 0.01$) (Fig. 3b). Those of CD44v6 positive cells in 3D (13.00 ± 1.14)% and in 2D (3.98 ± 0.41)% were both higher than those of the isotype control (0.40 ± 0.06)% (Fig. 3c–c″) and in 3D they were significantly higher than in 2D ($^{**}P < 0.01$) (Fig. 3d). The percentages of CD133 positive cells in 3D (18.18 ± 1.87)% and in 2D (8.23 ± 0.95)% were both higher than those of the isotype control (0.32 ± 0.03)% (Fig. 3e–e″) and in 3D they were significantly higher than in 2D ($^{**}P < 0.01$) (Fig. 3f).

As shown in Fig. 4 after flow cytometry, in PANC-1, the percentages of CD44 positive cells in 3D (15.51 ± 1.62)% and in 2D (4.67 ± 0.65)% were both higher than those of the isotype control (0.09 ± 0.01)% (Fig. 4a–a″) and in 3D they were significantly higher than in 2D ($^{**}P < 0.01$) (Fig. 4b). Those of CD44v6 positive cells in 3D (9.10 ± 1.03)% and in 2D (2.14 ± 0.21)% were both higher than those of the isotype control (0.48 ± 0.05)% (Fig. 4c–c″) and in 3D they were significantly higher than in 2D ($^{**}P < 0.01$) (Fig. 4d). Those of CD133 positive cells in 3D (14.29 ± 1.38)% and in 2D (5.42 ± 0.72)% were both higher than those of the isotype control (0.69 ± 0.04)% (Fig. 4e–e″) and in 3D they were significantly higher than in 2D ($^{**}P < 0.01$) (Fig. 4f).

As shown in Fig. 5, in PC3, the percentages of CD44 positive cells in 3D (13.85 ± 1.22)% and in 2D (2.36 ± 0.53)% were both higher than those of the isotype control (0.26 ± 0.05)% (Fig. 5a–a″) and in 3D they were significantly higher than in 2D ($^{**}P < 0.01$) (Fig. 5b). Those of CD44v6 positive cells in 3D (10.76 ± 1.04)% and in 2D (1.23 ± 0.12)% were both higher than those of the isotype control (0.11 ± 0.04)% (Fig. 5c–c″) and in 3D they were significantly higher than in 2D ($^{**}P < 0.01$) (Fig. 5d). The percentages of CD133 positive cells in 3D (12.90 ± 1.18)% and in 2D (3.85 ± 0.39)% were higher than those of the isotype control (0.67 ± 0.06)% (Fig. 5e–e″) and in 3D they were significantly higher than in 2D ($^{**}P < 0.01$) (Fig. 5f).

As shown in Fig. 6, in OVCAR-3, the percentages of CD44 and CD133 double positive cells in 3D (7.23 ± 0.72)% and in 2D (3.02 ± 0.26)% were both higher than those of the isotype control (0.00 ± 0.00)% (Fig. 6a) and in 3D they were significantly higher than in 2D ($^{**}P < 0.01$) (Fig. 6b). In SW620, the percentages of CD44 and CD133 double positive cells in 3D (5.59 ± 0.68)% and in 2D (3.66 ± 0.28)% were both higher than those of the isotype control (0.00 ± 0.00)% (Fig. 6a′) and in 3D they were significantly higher than that in 2D ($^{**}P < 0.01$) (Fig. 6b′). In PANC-1, the percentages of CD44 and CD133 double positive cells in 3D (10.61 ± 1.08)% and in 2D (2.11 ± 0.18)% were both higher than those of the isotype control (0.00 ± 0.00)% (Fig. 6a″) and in 3D they were significantly higher than in 2D ($^{**}P < 0.01$) (Fig. 6b″). In PC3, the percentages of CD44 and CD133 double positive cells in 3D (6.30 ± 0.70)% and in 2D (2.01 ± 0.16)% were both higher than those of the isotype control (0.01 ± 0.00)% (Fig. 6a‴) and in 3D they were significantly higher than in 2D ($^{**}P < 0.01$) (Fig. 6b‴).

These data demonstrated that some CSCs could be enriched through agarose multi-well dishes using rubber micro-molds to make cancer cells into 3D spheroids.

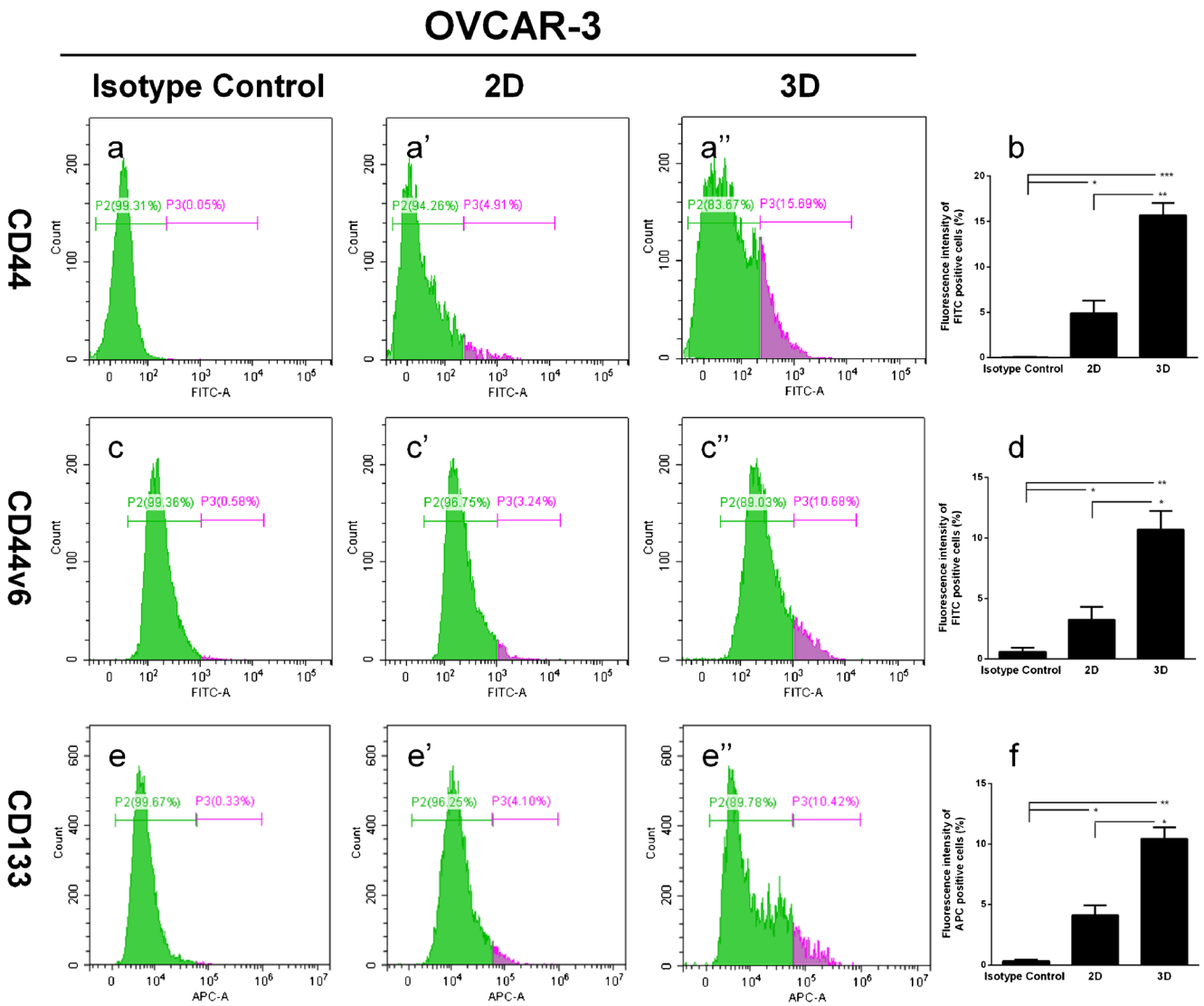

Fig. 2 Flow cytometry comparative analysis of cancer stem cell biomarker expression in 2D and 3D human ovarian mucosal cells (OVCAR-3). (a–a″). Flow cytometry comparative analysis of the cell ratio of expression CD44 in 2D and 3D OVCAR-3. (b) Quantification of the flow cytometry results for CD44. (c–c″). Flow cytometry comparative analysis of the cell ratio of expression CD44v6 in 2D and 3D OVCAR-3. (d) Quantification of the flow cytometry results for CD44v6. (e–e″). Flow cytometry comparative analysis of the cell ratio of expression CD133 in 2D and 3D OVCAR-3. (f) Quantification of the flow cytometry results for CD133. Mean ± SE, $n = 3$. Differences with $^{*}P < 0.05$, $^{**}P < 0.01$ and $^{***}P < 0.001$ were considered statistically significant

Protein and gene expression levels of OCT4 in 2D and 3D cancer cells

In order to maintain stemness, the expression levels of stemness transcription factors in stem cells were much higher than those of adult cells. Stemness transcription factors such as OCT4, NANOG and SOX2 play key roles in the process of adult cells reprogrammed into stem cells. CSCs and normal adult stem cells have the same characteristics of self-renewal and multi-directional differentiation potential (Clarke et al. 2006). We examined the expression of the basic stem cell profile of OCT4, NANOG and SOX2 in cancer cells cultured in different states. Western blot was conducted to detect the OCT4, NANOG and SOX2 expressions in 2D and 3D human ovarian mucosal cells (OVCAR-3), human colon cancer cells (SW620), human pancreatic cancer cells (PANC-1) and human prostate cancer cells (PC3) (Fig. 7a). The results showed that the OCT4, NANOG and SOX2 protein expression levels in all 3D cancer cells including OVCAR-3, SW620, PANC-1 and PC3 were significantly higher than that in 2D (Fig. 7b–b″).

In addition, the results of qPCR also demonstrated that *Oct4, Nanog and Sox2* gene expression levels in all 3D cancer cells, including OVCAR-3, SW620, PANC-1 and PC3 were significantly higher than that in 2D (Fig. 7c–c″).

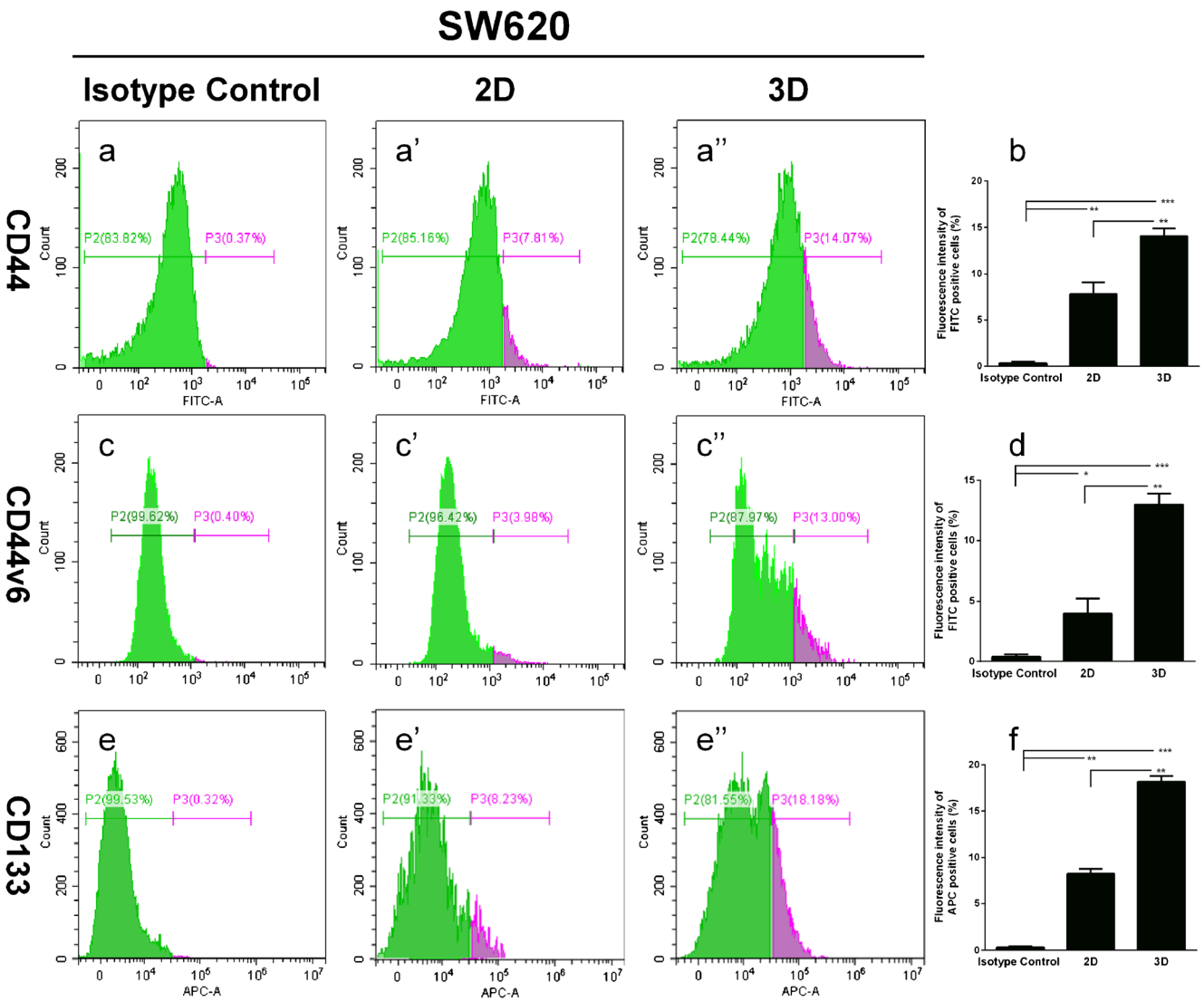

Fig. 3 Flow cytometry comparative analysis of cancer stem cell biomarker expression in 2D and 3D human colon cancer cells (SW620). (a–a″) Flow cytometry comparative analysis of the cell ratio of expression CD44 in 2D and 3D SW620. (b) Quantification of the flow cytometry results for CD44. (c–c″) Flow cytometry comparative analysis of the cell ratio of expression CD44v6 in 2D and 3D SW620. (d) Quantification of the flow cytometry results for CD44v6. (e–e″) Flow cytometry comparative analysis of the cell ratio of expression CD133 in 2D and 3D SW620. (f) Quantification of the flow cytometry results for CD133. Mean ± SE, $n = 3$. Differences with $^{*}P < 0.05$, $^{**}P < 0.01$ and $^{***}P < 0.001$ were considered statistically significant

These results further suggest that CSCs can be enriched through agarose multi-well dishes using rubber micro-molds to make cancer cells into 3D spheroids.

The colony formation of cancer cells in 3D

The main characteristic of CSCs is its ability to form new tumors in murine models or colonies in soft agar. We seeded the cancer cells from 3D into a medium with 0.3% soft agar. On day 14, there were colonies with different sizes of formation in the 3D cancer cells and very few dissociated cells suspended in the medium. Meanwhile, the mean size of colonies in PANC-1 seemed bigger than that of others (Fig. 7d–d″′). These results demonstrated that CSCs that were enriched through agarose multi-well dishes using rubber micro-molds to make cancer cells into 3D spheroids had the ability to form colonies in soft agar.

Discussion

CSCs, also known as tumor-initiating cells, are capable of self-renewing and maintaining their stemness, differentiating into cancer cells and playing a core role in tumorigenesis, metastasis and therapy resistance (Jin et al. 2017). Developing therapeutic strategies that not only kill cancer cells but also eliminate CSCs has potential for achieving better treatment outcomes (Zhou et al. 2017). Thus, further study is

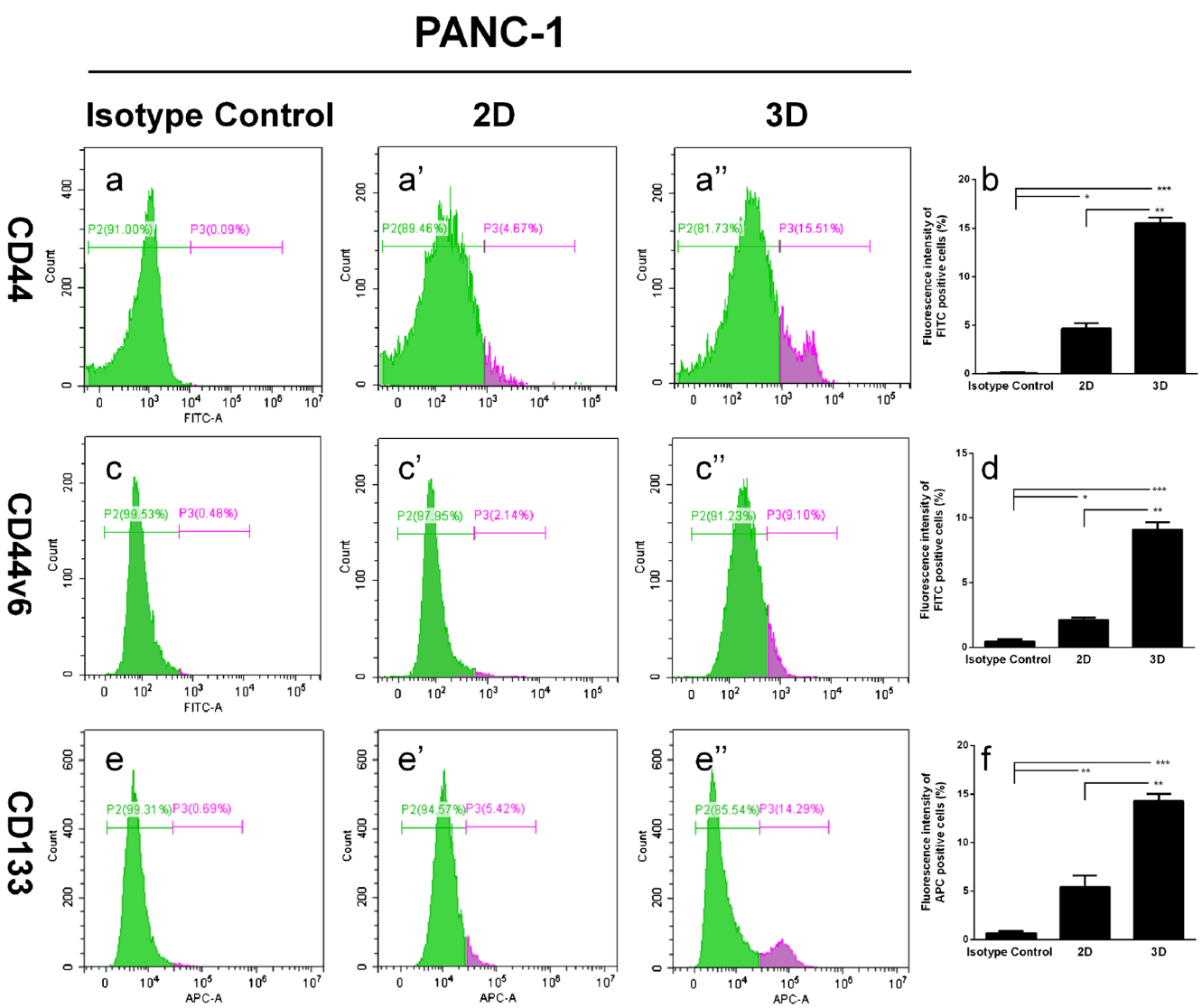

Fig. 4 Flow cytometry comparative analysis of cancer stem cell biomarker expression in 2D and 3D human pancreatic cancer cells (PANC-1). (a–a″) Flow cytometry comparative analysis of the cell ratio of expression CD44 in 2D and 3D PANC-1. (b) Quantification of the flow cytometry results for CD44. (c–c″) Flow cytometry comparative analysis of the cell ratio of expression CD44v6 in 2D and 3D PANC-1. d Quantification of the flow cytometry results for CD44v6. (e–e″) Flow cytometry comparative analysis of the cell ratio of expression CD133 in 2D and 3D PANC-1. (f) Quantification of the flow cytometry results for CD133. Mean ± SE, $n = 3$. Differences with $^{*}P < 0.05$, $^{**}P < 0.01$ and $^{***}P < 0.001$ were considered statistically significant

needed to firstly explore the novel and rapid enrichment methods of CSCs for targeted therapy researches. In this study, we reported a new approach to rapidly enrich CSCs in certain cancer cells, such as human ovarian mucosal cells (OVCAR-3), human colon cancer cells (SW620), human pancreatic cancer cells (PANC-1) and human prostate cancer cells (PC3).

Recently, spheroid culture (3D) has been increasingly used as a method for enriching stem cells, which relies on their property of anchorage independent growth. Growing cells in a 3D environment generated important differences in cellular characteristics and behaviors compared with conventional adherent culture (2D) (Page et al. 2013). Researchers have reported the application of spheroid culture to isolate, enrich, maintain, or expand potential CSC subpopulations from various types of cancers (Fujii et al. 2009; Gou et al. 2007; Ponti et al. 2005). To our knowledge, there have been few reports on the rapid enrichment and long-term propagation (at least culture passage five times with an appreciable stemness in this study and data not shown) of CSCs through agarose multi-well dishes using rubber micro-molds to make cancer cells into 3D spheroids. 3D culture might form a distinct extracellular matrix (ECM) and establish new cell-matrix interactions to influence cell fate and improve cell activity (Garcion et al. 2004; Huang et al. 2013; Song et al. 2002). ECM can influence cell adhesion, proliferation and stemness and it contains various compositions and architectures (Rao Pattabhi et al. 2014). ECM derived from some special cells efficiently

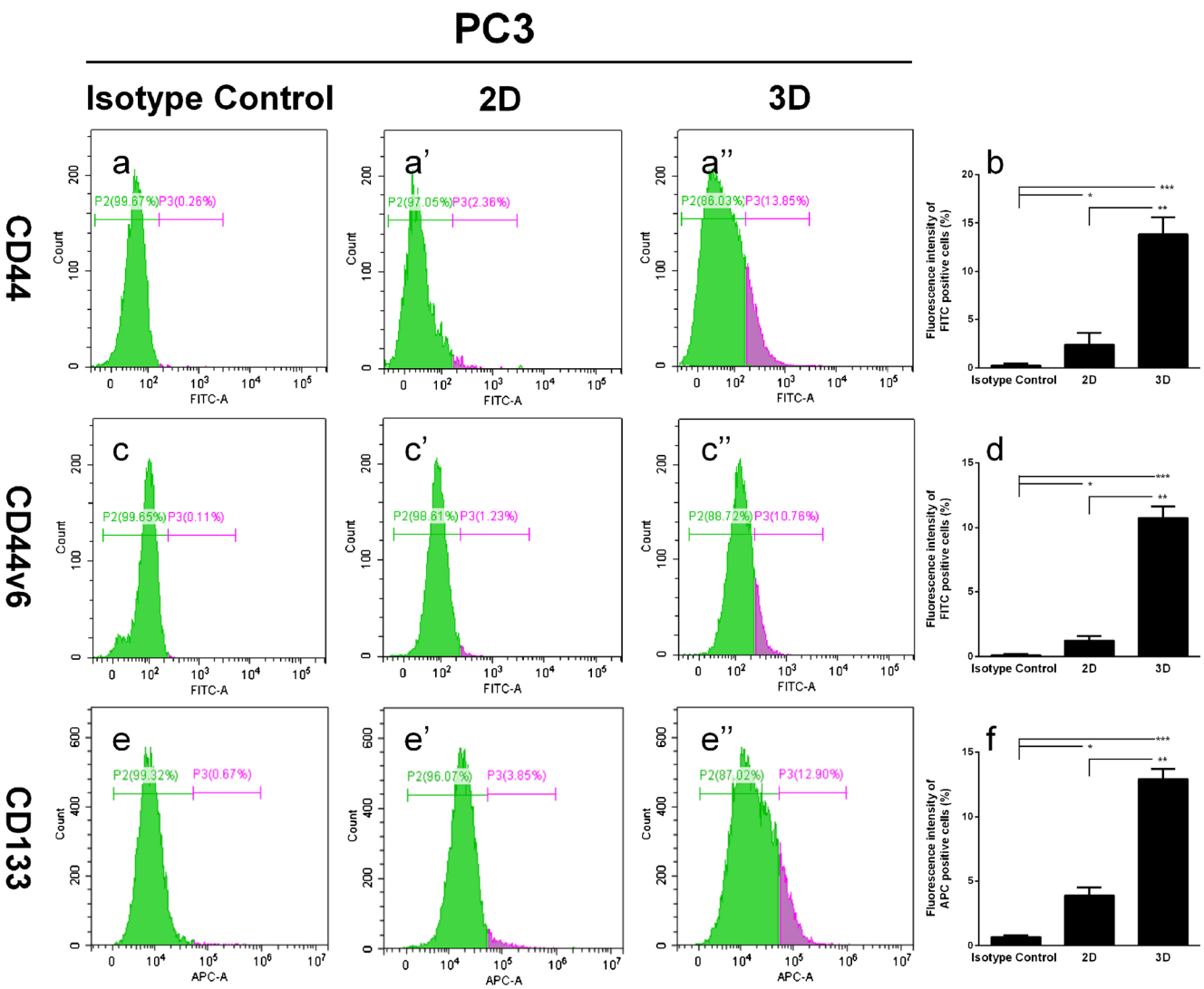

Fig. 5 Flow cytometry comparative analysis of cancer stem cell biomarker expression in 2D and 3D human prostate cancer cells (PC3). (a–a″) Flow cytometry comparative analysis of the cell ratio of expression CD44 in 2D and 3D PC3. (b) The quantification of the flow cytometry results for CD44. (c–c″) Flow cytometry comparative analysis of the cell ratio of expression CD44v6 in 2D and 3D PC3. (d) Quantification of the flow cytometry results for CD44v6. (e–e″) Flow cytometry comparative analysis of the cell ratio of expression CD133 in 2D and 3D PC3. (f) Quantification of the flow cytometry results for CD133. Mean ± SE, $n = 3$. Differences with $^{*}P < 0.05$, $^{**}P < 0.01$ and $^{***}P < 0.001$ were considered statistically significant

maintain the stemness of stem cells or ameliorate the stemness deprivation primarily through the Wnt pathway (Lee et al. 2017a; Xiong et al. 2015; Zhang et al. 2018). In order to avoid the dependence on trophoblast cells for embryonic stem cell (ESC) culture, even for induced pluripotent stem cell (iPSC) culture at present, the culture dishes must be coated with ECM-named matrigel in advance for cell adhesion and stemness maintenance (Guo et al. 2015b). Our previous works also confirmed that spheroid cultures promoted cellular stemness and viability in bovine corneal endothelial cells (B-CECs) and corneal stromal cells (CSCs) (Guo et al. 2015a; Guo et al. 2015c).

Based on cell surface biomarkers, CSCs are isolated from cell lines of different cancer types as well as patient tissues. CD44 is a widely expressed polymorphic integral membrane adhesion molecule that binds hyaluronic acid and contributes to cell-cell and cell matrix adhesion interactions, which is involved in cancer cell migration, proliferation and metastasis (Orian-Rousseau 2010). CD44 transcripts undergo complex alternative splicing, resulting in functionally different isoforms. The standard isoform (CD44s) has been more extensively researched and the variant isoforms (CD44v) seem restricted to subpopulations endowed with stem cell potential and cancer development. Among CD44v isoforms, CD44v6 plays a major role in cancer cell migration and invasion (Todaro et al. 2014). CD133 (prominin-1), a 5-transmembrane glycoprotein, is a novel pentaspan membrane protein and has recently been considered to be an important marker of CSCs in many kinds of

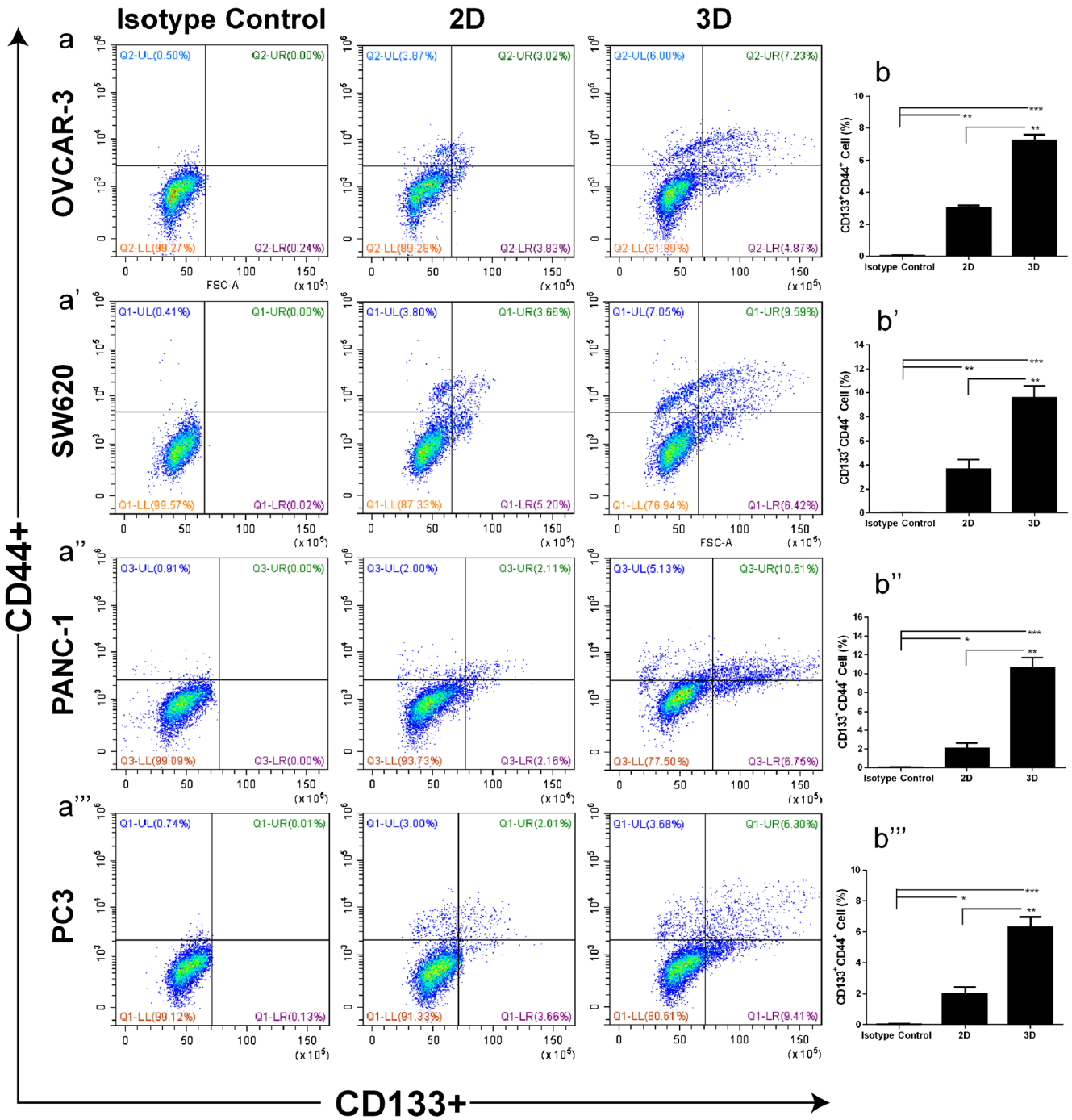

Fig. 6 Flow cytometry double-label analysis of cancer stem cell biomarker expression in 2D and 3D of OVCAR-3, OVCAR-3, PANC-1 and PC3. (a–a‴) Flow cytometry comparative analysis of both CD44 and CD133 positive cell ratios in 2D and 3D of OVCAR-3, OVCAR-3, PANC-1 and PC3. (b–b‴) Quantification of the flow cytometry double-label analysis results. Mean ± SE, $n = 3$. Differences with $^{*}P < 0.05$, $^{**}P < 0.01$ and $^{***}P < 0.001$ were considered statistically significant

cancer cell lineages, including the brain, colon, ovarian, pancreatic and prostate cancers. Patients with high levels of CD133 expression have a poor prognosis (Jin et al. 2017). Recently, numerous research groups reported that CSCs could be successfully isolated by these cell surface phenotypes (Heider et al. 2004; Zhu et al. 2010). The CSCs of cancer cells (OVCAR-3, SW620, PANC-1 and PC3) all expressed CD44, CD44v6 and CD133 (Collins et al. 2005; Du et al. 2008; Hermann et al. 2007; Kryczek et al. 2012; Li et al. 2009; Meirelles et al. 2012; O'Brien et al. 2007). Nevertheless, in our study, the single and double stain of flow cytometry was used to assess the CSC proportions of different cancer cells with 3D culture based on expression of

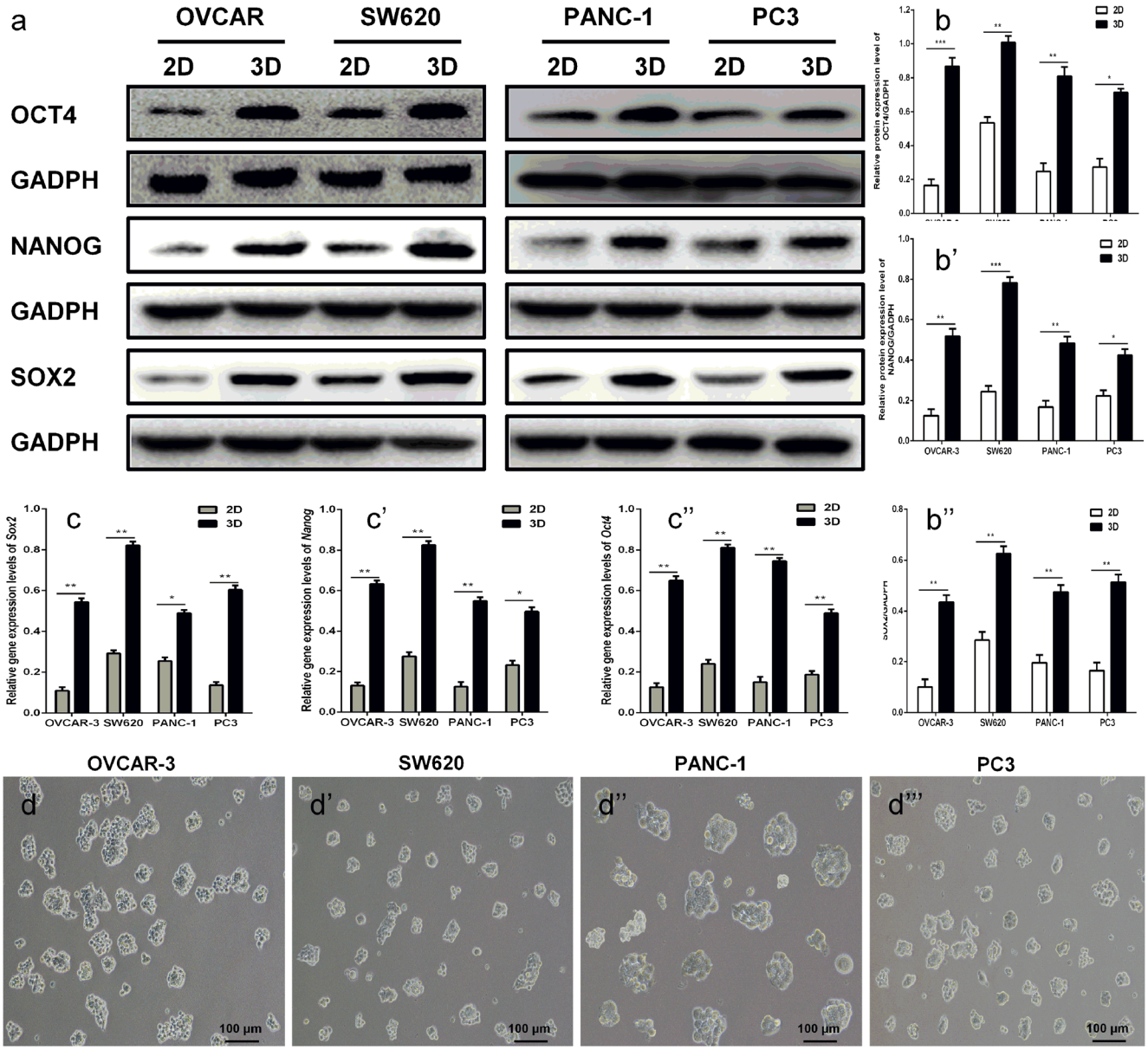

Fig. 7 The protein and gene expression levels of stemness transcription factors in 2D and 3D cancer cells. (a) Western blot band of OCT4, NANOG, and SOX2 in 2D and 3D cancer cells. (b–b″) Quantification of protein levels. (c–c″) Quantitative polymerase chain reaction (qPCR) of *Oct4 Nanog, and Sox2* in 2D and 3D cancer cells. (d–d″) The images of 3D cancer cell colonies under an invert optical microscope. Mean ± SE, $n = 3$. Differences with $^{*}P < 0.05$, $^{**}P < 0.01$, and $^{***}P < 0.001$ were considered statistically significant. *Scale bars* 100 μm

potential CSC-markers of CD44, CD44v6 and CD133 or both CD44 and CD133, which showed that cancer cells in 3D had more CSCs than those in 2D.

CSCs and normal adult stem cells have the same characteristics, namely having self-renewal and multi-directional differentiation potential (Clarke et al. 2006). OCT4, NANOG and SOX2, the mammalian stemness transcription factors, are mainly expressed in the pluripotent cells of an embryo, cell lines and the germ cells (GCs), which play a core part in a regulatory system of reprogramming adult cells into stem cells and maintain stemness (Kim et al. 2009). To confirm the stem cell phenotype of 3D cancer cells, the expressions of OCT4, NANOG and SOX2 were evaluated. The results of Western blot and qPCR revealed that OCT4, NANOG and SOX2 expression levels of cancer cells (OVCAR-3, SW620, PANC-1 and PC3) in 3D were significantly higher than those in 2D. In addition, the main characteristic of CSCs is its ability to form new tumors in murine models or side population (Xu et al. 2014). In this study, the CSCs through cell spheroids (3D) using rubber micro-molds could form colonies with different sizes in soft agar. These data suggest that CSCs could be enriched through a 3D spheroid culture based on this method.

In conclusion, our results displayed a new method to enrich a certain amount of CSCs from cancer cells (OVCAR-3,

SW620, PANC-1 and PC3) through agarose multi-well dishes using rubber micro-molds to make cancer cells into 3D spheroids, which might be of benefit for CSC-targeted therapy studies and anti-CSC drug screening applications in the future. Meanwhile, based on this method, the controllable cancer cell spheroids with unified size could be rapidly produced and used to transplant into the body of animals to establish tumor models for drug screening.

Funding This work was supported by the National Nature Science Foundation of China (81701426, 81730042 and 81771636), the Medical and Health Research Science and Technology Plan Project of Zhejiang Province (2018KY523, 2017KY473 and 2017ZB067) and the Public Welfare Science and Technology Plan Project of Wenzhou City (Y20170151, Y20160069 and ZS2017012).

Compliance with ethical standards

Conflict of interest The authors declare that they have no conflict of interest.

References

Al-Hajj M, Wicha MS, Benito-Hernandez A, Morrison SJ, Clarke MF (2003) Prospective identification of tumorigenic breast cancer cells. Proc Natl Acad Sci U S A 100:3983–3988

Bhaskara VK, Mohanam I, Rao JS, Mohanam S (2012) Intermittent hypoxia regulates stem-like characteristics and differentiation of neuroblastoma cells. PLoS One 7:e30905

Bonnet D, Dick JE (1997) Human acute myeloid leukemia is organized as a hierarchy that originates from a primitive hematopoietic cell. Nat Med 3:730–737

Cao L, Zhou Y, Zhai B, Liao J, Xu W, Zhang R, Li J, Zhang Y, Chen L, Qian H, Wu M, Yin Z (2011) Sphere-forming cell subpopulations with cancer stem cell properties in human hepatoma cell lines. BMC Gastroenterol 11:71

Chien CY, Chuang HC, Chen CH (2012) The side population of cancer stem-like cells in human oral cancer. Oral Oncol 48:913–914

Clarke MF, Dick JE, Dirks PB, Eaves CJ, Jamieson CH, Jones DL, Visvader J, Weissman IL, Wahl GM (2006) Cancer stem cells–perspectives on current status and future directions: AACR workshop on cancer stem cells. Cancer Res 66:9339–9344

Collins AT, Berry PA, Hyde C, Stower MJ, Maitland NJ (2005) Prospective identification of tumorigenic prostate cancer stem cells. Cancer Res 65:10946–10951

Du L, Wang H, He L, Zhang J, Ni B, Wang X, Jin H, Cahuzac N, Mehrpour M, Lu Y, Chen Q (2008) CD44 is of functional importance for colorectal cancer stem cells. Clin Cancer Res : Off J Am Assoc Cancer Res 14:6751–6760

Fujii H, Honoki K, Tsujiuchi T, Kido A, Yoshitani K, Takakura Y (2009) Sphere-forming stem-like cell populations with drug resistance in human sarcoma cell lines. Int J Oncol 34:1381–1386

Garcion E, Halilagic A, Faissner A, ffrench-Constant C (2004) Generation of an environmental niche for neural stem cell development by the extracellular matrix molecule tenascin C. Development 131:3423–3432

Gou S, Liu T, Wang C, Yin T, Li K, Yang M, Zhou J (2007) Establishment of clonal colony-forming assay for propagation of pancreatic cancer cells with stem cell properties. Pancreas 34:429–435

Guo X, Li S, Ji Q, Lian R, Chen J (2015a) Enhanced viability and neural differential potential in poor post-thaw hADSCs by agarose multi-well dishes and spheroid culture. Hum Cell 28:175–189

Guo X, Lian R, Guo Y, Liu Q, Ji Q, Chen J (2015b) bFGF and Activin A function to promote survival and proliferation of single iPS cells in conditioned half-exchange mTeSR1 medium. Hum Cell 28:122–132

Guo Y, Liu Q, Yang Y, Guo X, Lian R, Li S, Wang C, Zhang S, Chen J (2015c) The effects of ROCK inhibitor Y-27632 on injectable spheroids of bovine corneal endothelial cells. Cell Reprogram 17:77–87

Heider KH, Kuthan H, Stehle G, Munzert G (2004) CD44v6: a target for antibody-based cancer therapy. Cancer Immunol, Immunother: CII 53:567–579

Hermann PC, Huber SL, Herrler T, Aicher A, Ellwart JW, Guba M, Bruns CJ, Heeschen C (2007) Distinct populations of cancer stem cells determine tumor growth and metastatic activity in human pancreatic cancer. Cell Stem Cell 1:313–323

Hu X, Ghisolfi L, Keates AC, Zhang J, Xiang S, Lee DK, Li CJ (2012) Induction of cancer cell stemness by chemotherapy. Cell Cycle 11:2691–2698

Huang YC, Chan CC, Lin WT, Chiu HY, Tsai RY, Tsai TH, Chan JY, Lin SJ (2013) Scalable production of controllable dermal papilla spheroids on PVA surfaces and the effects of spheroid size on hair follicle regeneration. Biomaterials 34:442–451

Jemal A, Bray F, Center MM, Ferlay J, Ward E, Forman D (2011) Global cancer statistics. CA Cancer J Clin 61:69–90

Jin X, Jin X, Kim H (2017) Cancer stem cells and differentiation therapy. Tumour Biol: J Int Socr Oncodev Biol Med 39:1010428317729933

Kim JB, Sebastiano V, Wu G, Arauzo-Bravo MJ, Sasse P, Gentile L, Ko K, Ruau D, Ehrich M, van den Boom D, Meyer J, Hubner K, Bernemann C, Ortmeier C, Zenke M, Fleischmann BK, Zaehres H, Scholer HR (2009) Oct4-induced pluripotency in adult neural stem cells. Cell 136:411–419

Kryczek I, Liu S, Roh M, Vatan L, Szeliga W, Wei S, Banerjee M, Mao Y, Kotarski J, Wicha MS, Liu R, Zou W (2012) Expression of aldehyde dehydrogenase and CD133 defines ovarian cancer stem cells. Int J Cancer 130:29–39

Lee MK, Lin SP, HuangFu WC, Yang DS, Liu IH (2017a) Endothelial-derived extracellular matrix ameliorate the stemness deprivation during ex vivo expansion of mouse bone marrow-derived mesenchymal stem cells. PLoS One 12:e0184111

Lee SY, Jeong EK, Ju MK, Jeon HM, Kim MY, Kim CH, Park HG, Han SI, Kang HS (2017b) Induction of metastasis, cancer stem cell phenotype, and oncogenic metabolism in cancer cells by ionizing radiation. Mol Cancer 16:10

Li C, Lee CJ, Simeone DM (2009) Identification of human pancreatic cancer stem cells. Methods Mol Biol 568:161–173

Lopez J, Poitevin A, Mendoza-Martinez V, Perez-Plasencia C, Garcia-Carranca A (2012) Cancer-initiating cells derived from established cervical cell lines exhibit stem-cell markers and increased radioresistance. BMC Cancer 12:48

Meirelles K, Benedict LA, Dombkowski D, Pepin D, Preffer FI, Teixeira J, Tanwar PS, Young RH, MacLaughlin DT, Donahoe PK, Wei X (2012) Human ovarian cancer stem/progenitor cells are stimulated by doxorubicin but inhibited by Mullerian inhibiting substance. Proc Natl Acad Sci U S A 109:2358–2363

O'Brien CA, Pollett A, Gallinger S, Dick JE (2007) A human colon cancer cell capable of initiating tumour growth in immunodeficient mice. Nature 445:106–110

Orian-Rousseau V (2010) CD44, a therapeutic target for metastasising tumours. Eur J Cancer 46:1271–1277

Page H, Flood P, Reynaud EG (2013) Three-dimensional tissue cultures: current trends and beyond. Cell Tissue Res 352:123–131

Peitzsch C, Tyutyunnykova A, Pantel K, Dubrovska A (2017) Cancer stem cells: the root of tumor recurrence and metastases. Semin Cancer Biol 44:10–24

Ponti D, Costa A, Zaffaroni N, Pratesi G, Petrangolini G, Coradini D, Pilotti S, Pierotti MA, Daidone MG (2005) Isolation and in vitro propagation of tumorigenic breast cancer cells with stem/progenitor cell properties. Cancer Res 65:5506–5511

Rao Pattabhi S, Martinez JS, Keller TC 3rd (2014) Decellularized ECM effects on human mesenchymal stem cell stemness and differentiation. Differentiation 88:131–143

Ricci-Vitiani L, Lombardi DG, Pilozzi E, Biffoni M, Todaro M, Peschle C, De Maria R (2007) Identification and expansion of human colon-cancer-initiating cells. Nature 445:111–115

Salmanzadeh A, Romero L, Shafiee H, Gallo-Villanueva RC, Stremler MA, Cramer SD, Davalos RV (2012) Isolation of prostate tumor initiating cells (TICs) through their dielectrophoretic signature. Lab Chip 12:182–189

Schatton T, Murphy GF, Frank NY, Yamaura K, Waaga-Gasser AM, Gasser M, Zhan Q, Jordan S, Duncan LM, Weishaupt C, Fuhlbrigge RC, Kupper TS, Sayegh MH, Frank MH (2008) Identification of cells initiating human melanomas. Nature 451: 345–349

Sell S (2004) Stem cell origin of cancer and differentiation therapy. Crit Rev Oncol Hematol 51:1–28

Singh SK, Clarke ID, Terasaki M, Bonn VE, Hawkins C, Squire J, Dirks PB (2003) Identification of a cancer stem cell in human brain tumors. Cancer Res 63:5821–5828

Song X, Zhu CH, Doan C, Xie T (2002) Germline stem cells anchored by adherens junctions in the Drosophila ovary niches. Science 296: 1855–1857

Takaishi S, Okumura T, Tu S, Wang SS, Shibata W, Vigneshwaran R, Gordon SA, Shimada Y, Wang TC (2009) Identification of gastric cancer stem cells using the cell surface marker CD44. Stem Cells 27: 1006–1020

Todaro M, Gaggianesi M, Catalano V, Benfante A, Iovino F, Biffoni M, Apuzzo T, Sperduti I, Volpe S, Cocorullo G, Gulotta G, Dieli F, De Maria R, Stassi G (2014) CD44v6 is a marker of constitutive and reprogrammed cancer stem cells driving colon cancer metastasis. Cell Stem Cell 14:342–356

Velasco-Velazquez MA, Homsi N, De La Fuente M, Pestell RG (2012) Breast cancer stem cells. Int J Biochem Cell Biol 44:573–577

Wang YC, Yo YT, Lee HY, Liao YP, Chao TK, Su PH, Lai HC (2012) ALDH1-bright epithelial ovarian cancer cells are associated with CD44 expression, drug resistance, and poor clinical outcome. Am J Pathol 180:1159–1169

Wang D, Plukker JTM, Coppes RP (2017) Cancer stem cells with increased metastatic potential as a therapeutic target for esophageal cancer. Semin Cancer Biol 44:60–66

Xiong Y, He J, Zhang W, Zhou G, Cao Y, Liu W (2015) Retention of the stemness of mouse adipose-derived stem cells by their expansion on human bone marrow stromal cell-derived extracellular matrix. Tissue Eng A 21:1886–1894

Xu XX, Liu C, Liu Y, Yang L, Li N, Guo X, Sun GW, Ma XJ (2014) Enrichment of cancer stem cell-like cells by culture in alginate gel beads. J Biotechnol 177:1–12

Zhang Y, Wang Z, Yu J, Shi J, Wang C, Fu W, Chen Z, Yang J (2012) Cancer stem-like cells contribute to cisplatin resistance and progression in bladder cancer. Cancer Lett 322:70–77

Zhang CL, Huang T, Wu BL, He WX, Liu D (2017) Stem cells in cancer therapy: opportunities and challenges. Oncotarget 8:75756–75766

Zhang JC, Song ZC, Xia YR, Shu R (2018) Extracellular matrix derived from periodontal ligament cells maintains their stemness and enhances redifferentiation via the wnt pathway. J Biomed Mater Res A 106:272–284

Zhou G, Latchoumanin O, Bagdesar M, Hebbard L, Duan W, Liddle C, George J, Qiao L (2017) Aptamer-based therapeutic approaches to target cancer stem cells. Theranostics 7:3948–3961

Zhu Z, Hao X, Yan M, Yao M, Ge C, Gu J, Li J (2010) Cancer stem/progenitor cells are highly enriched in CD133+CD44+ population in hepatocellular carcinoma. Int J Cancer 126:2067–2078